Engineering Transactions, **74**(1): 19–38, 2026, https://doi.org/10.24423/engtrans.2025.3561
Institute of Fundamental Technological Research Polish Academy of Sciences (IPPT PAN)
Université de Lorraine • Poznan University of Technology

Research Paper

Evaluation of the Characteristics and Application of SBS Composite-Modified Bitumen Materials in Low-Temperature Environments

Wenxiao REN[1),2)], Ping LI[1)*]

[1)] *School of Civil Engineering, Lanzhou University of Technology*
Lanzhou, China

[2)] *School of Civil Engineering, Northwest Minzu University*
Lanzhou, China

[*]Corresponding Author: lzlgliping@126.com

To improve the resistance of bitumen pavements to low-temperature cracking, this study proposes a composite-modified bitumen based on styrene-butadiene-styrene (SBS) copolymer and crumb rubber. This modified bitumen is also tested for its performance in a low-temperature environment. The test results indicate that, after aging and freeze-thaw cycles (FTCs), the creep rates (CRs) of both SBS-modified bitumen and the SBS/crumb rubber composite-modified bitumen decreased. However, the CR of the SBS/crumb rubber composite-modified bitumen was constantly lower than that of the SBS-modified bitumen. For example, at $-12\,^{\circ}\mathrm{C}$, the CRs of the aged SBS-modified bitumen and SBS/crumb rubber composite-modified bitumen were 0.44 and 0.37, respectively. When the bitumen mixtures underwent FTCs and aging, their fracture energy densities (FEDs) drastically decreased. Nevertheless, the FEDs of the SBS/crumb rubber composite-modified bitumen mixtures were higher than those of the SBS-modified bitumen mixtures. These results indicate that the composite-modified bitumen with SBS/crumb rubber has good rheological properties and freeze-thaw resistance, thereby effectively ensuring the low-temperature performance of bitumen pavements.

Keywords: SBS, modified bitumen, rheological properties, low-temperature properties, freeze–thaw cycles (FTCs), crumb rubber.

1. Introduction

As the most common pavement surfacing material, bitumen pavement (AP), compared with other pavements, has the advantages of a smooth surface, comfortable driving, and easy maintenance and repair. However, in low-temperature (LT) environments, the bitumen binding material is prone to cracking, which seriously affects the performance and life of AP [1, 2]. The LT cracking problem of AP can be improved by enhancing the rheological properties of bitumen. One

typical bitumen modification that can successfully increase the ductility and viscoelasticity of bitumen while lowering its temperature sensitivity is styrene butadiene styrene copolymer (SBS copolymer) [3, 4].

In the 1840s, researchers first attempted to mix natural rubber into base bitumen to prepare modified bitumen. Later, synthetic rubber and natural rubber were used to modify base bitumen. However, it was not until the 1930s that the preparation process of rubber-modified bitumen was more effectively improved. In the 1960s, rubber powder obtained from waste tires began to be added to base bitumen in some countries to prepare rubberized bitumen and apply it to road construction. However, due to the poor compatibility between rubber powder and bitumen, many undispersed rubber particles remain, resulting in disadvantages such as high viscosity, poor flowability, and poor dispersibility of bitumen. Liu *et al.* [5] proposed a method of using carbon nanotubes (CNTs) mixed with SBS-modified bitumen to address the issue of early damage to bitumen pavements. Their study analyzed the effects of different CNT concentrations on the high-temperature (HT) and LT performance, as well as the aging behavior of SBS-A, through a series of experiments. The results showed that the optimal concentration of CNTs was 1 %, and the changes in modified bitumen during aging were analyzed by infrared spectroscopy. Ting *et al.* [6] proposed a composite modified asphalt (MA) based on SBS and methylene diphenyl diisocyanate (MDI) to address the problem of poor stability of SBS-MA. MDI, according to the experimental findings, acted as a phase compatibilizer between bitumen and SBS, improving the composite-modified phase stability of bitumen while decreasing its chemical softness and polarizability. Duarte Mendonça *et al.* [7] addressed the problem of how to improve the elasticity of bitumen by proposing a lignin-based MA. According to the testing results, the addition of 3 % pine lignin and 9 % eucalyptus lignin produced bitumen with the best mechanical qualities, indicating that lignin is an excellent alternative to synthetic elastomeric polymers.

To address the issue of how to enhance the HT and LT properties as well as the water stability of bitumen, Li *et al.* [8] presented an MA based on bamboo fiber. According to the experimental findings, bamboo fiber MA blends performed better in terms of HT, LT, and water stability compared with SBS-MA. With a fiber length of 7.25 mm and a content of 0.22 %, the optimum performance of the bitumen was obtained. Amini *et al.* [9] proposed a composite MA based on titanium dioxide, aluminum trioxide, and multiwalled CNTs to improve rutting and fatigue resistance of bitumen. The experimental results indicated that this MA had higher viscosity, better aging resistance, and a fatigue life that was 1.7 times longer than that of ordinary bitumen. Chen *et al.* [10] proposed to improve the performance of SBS-modified bitumen by grinding molybdenum disulfide (MoS_2) with polyphosphoric acid (PPA) in cyclic oil and mechanically

activating the mixture to produce PPA-modified MoS_2 (OMS-PPA), which was then mixed with SBS-modified bitumen. The results showed that, compared with SA, the permeation temperature coefficient of SA-OMS decreased by 3.7 %, and that of 1-SA-OMS-PPA decreased even more, i.e., by 7.1 %. After short-term aging, the generation of carboxyl groups and the rate of hardness were significantly reduced.

In summary, the current research on MA has been quite effective, and many different types of MA have been developed. However, most of the research on MAs primarily focused on their mechanical properties, while their their freeze-thaw cycles (FTC) resistance was relatively neglected. In view of the latter issue, in order to improve the FTC resistance of bitumen and minimize the manufacturing cost of modified bitumen, the FTC performance of composite modified bitumen based on SBS and rubber powder is analyzed. Moreover, to evaluate the performance of the composite MA, the study also innovatively analyzes the rheological and LT properties of the MA from both macro- and fine-scale perspectives.

2. Methods and materials

Gram-refined bitumen was selected as the matrix bitumen (MaA) for the experiment. The SBS modifier used was 4303 star type. The rubber powder modifier consisted of 40-mesh (380 μm) rubber powder particles. The optimal dosages of the SBS modifier and rubber powder modifier were determined through experiments on three major indicators of bitumen: dynamic shear, bending, and rheology in the early stage. The dosages of the SBS modifier and rubber powder modifier were 3 % and 20 % of the mass of the matrix bitumen, respectively. SBS-MA was prepared by blending SBS modifier into MaA. SBS composite crumb rubber (CCR) MA was prepared by blending the SBS modifier and the crumb rubber modifier into MaA. The coarse and fine aggregates used in the preparation of the bitumen mixtures (AMs) were basalt, comprising 97 % of the total. The mineral powder was limestone – 3 % of the total and having a fineness of less than 0.075 mm. The optimum oil/gravel ratios for the preparation of AMs with SBS-modified bitumen and CCR bitumen were 5 % and 6 %, respectively. The so-called oil-stone ratio refers to the mass ratio of asphalt (oil content) to aggregate (stone content) in asphalt mixtures. It is an important parameter in the design of asphalt mixtures, which has a significant impact on their performance.

In preparing the AM specimens, the mixture was first pressed into 300 mm × 300 mm × 50 mm rutted specimens using the wheel milling method. Then, the rutted specimen was cut into 250 mm × 30 mm × 35 mm beams. Moreover, a 4 mm × 2 mm notch was cut at the midpoint of the beamlet for subsequent tests.

2.1. Experimental design

Long-term aging (LTA) test of bitumen: 50 g of SBS bitumen and CCR bitumen were each put into a sample tray, and then short-term aging was carried out using a rotating film oven, with the heating time of 5 h and temperature of 163 °C, with a rotating speed of 5.5 rad/min. Then, the aged bitumen was poured into a sample tray to achieve a thickness of 3.2 mm. Next, it was placed into a pressure aging vessel (PAV) for 20 h for LTA simulation. The PAV temperature was set at 100 °C and the pressure to 2.1 MPa [11]. When the aging was completed, the bitumen samples were removed and placed in a stainless steel cylinder with heating and stirring to remove air bubbles inside the bitumen.

LTA test of the mixture: first, the AM was baked in an oven for 4 h at 135 °C after being evenly spread at a thickness of 21 kg/m^2 in an enameled tray. Then, the mixture was pressed into rutting specimens using the wheel milling method and cut into small beams. Subsequently, the obtained trabecular specimens were placed in a HT and LT alternating box heated under forced ventilation for 120 h at a heating temperature of 85 °C [12]. After heating, the door of the box was opened, and the specimens were removed after cooling to room temperature.

Bitumen FTC test: first, 50 g of SBS bitumen and CCR bitumen were weighed and evenly spread in a stainless steel cylinder (diameter: 122 mm) to a thickness of 3.2 mm. Then, the stainless steel cylinder was filled with water and an 8 % salt solution until the bitumen was fully submerged. Next, the stainless steel cylinder was sealed using cling film and placed in a HT and LT alternating chamber for freeze-thaw cycling. The freezing temperature was set at −20 °C for 2 h, and the thawing temperature at 60 °C for 4 h. The number of FTCs was 5, 10, 15, and 20.

FTC test: the specimens were first placed in water or salt solution (8 %). Then, the specimens were evacuated using a vacuum extractor to a vacuum level of 97.3 kPa, and the specimens were immersed under vacuum conditions for 15 min. After this, atmospheric pressure was restored and the immersion was continued for an additional 1 h. Then, the specimens were taken out and placed in a specimen box, which was filled with water or the 8 % salt solution until the specimens were fully submerged. Next, they were placed in a HT and LT alternating chamber for FTC [13]. The freezing temperature and time were −20 °C for 8 h. The melting temperature and time were 60 °C for 16 h. The number of FTCs was 5, 10, 15 and 20.

2.2. Experimental design of rheological and physico-chemical properties

Bending creep strength test: the test equipment was a bending beam rheometer, and the test indices were stiffness modulus and creep rate (CR). The test temperatures were −24 °C, −18 °C, and −12 °C.

Infrared spectroscopic tests: infrared tests were performed on different specimens using a Fourier transform infrared (FTIR) spectrometer. The number of scans and spectral acquisition intervals were 32 cm^{-1} and 650 cm^{-1} to 4000 cm^{-1}, respectively, and the resolution was 4 cm^{-1}.

Contact angle measurement test: first, the bitumen was heated until it was molten, and then it was put on a slide. After that, the slide was heated on a hot plate and left to flow naturally. The heating temperature was 120 °C. After cooling, the bitumen was placed in a sealed container and set aside. Next, the basalt aggregate was cut into cubes with a side length of 1 cm and polished to a smooth surface. The polished basalt specimens were then placed in an oven for drying at 45 °C for 6 h [14]. After the basalt specimens cooled to room temperature, they were removed and placed in a sealed container for backup. Then, the contact angle of the specimens was measured by dropping a liquid drop onto the specimen surface to be tested using the probe of a contact angle measuring instrument.

Atomic force microscopy (AFM) test: for the test, the scanning mode of the AFM was PeakForce QNM, the scanning frequency was 0.977 Hz, the scanning range was 20 μm × 20 μm, and the probe used was Bruker RTESPA-150.

2.3. LT *cracking property test*

Constrained specimen temperature stress (CSTS) test: first, epoxy resin adhesive was utilized to bond the ends of the AM beamlet specimen to the ends of the test system. After the epoxy resin adhesive solidified, the specimen was kept at 5 °C for 6 h. Then, the specimen was cooled at a rate of 10 °C/h and the temperature-stress curve was measured until the specimen fracture.

Three-point bending test (TPBT): the specimen was placed flat in the bending test fixture to form a simply-supported beam, and a dynamic hydraulic servo universal testing machine was utilized to apply the load. The loading speed was 1 mm/min, the test temperature was −12 °C, and the acquisition frequency was 10 Hz. It should be mentioned that the specimen was first coated with matte white paint throughout the collecting procedure in order to prevent specimen reflection. Moreover, a roller was used to make black spots on the surface of the specimen as markers to ensure accurate data acquisition.

2.4. Anti-rutting test

Rutting plate specimens were prepared using the bitumen mixture and rutting tests were conducted using the SYD-0719C-2 fully automatic rutting tester. Constant wheel pressure and uniform wheel speed were maintained during the experimental loading process. The rutting plate specimen together with the test mold were placed on the testing device, with the test wheel placed at the center

of the specimen. The travel direction of the test wheel was consistent with the rolling direction, and the test duration was 1 h. The test was stopped when the rutting deformation reached 25 mm.

3. Results

3.1. LT rheological characterization of composite MA

To evaluate the rheological properties of CCR bitumen, flexural creep strength tests were conducted on virgin, aged, and FTC-treated MA. The specimens were analyzed using infrared spectroscopy. The basic properties of CCR bitumen are shown in Table 1.

Table 1. Basic properties of CCR bitumen.

Item	Unit	Value
Needle penetration	dmm	52.5
Softening point	°C	228
Ductility	cm	85.7

As can be seen in Table 1, the penetration, softening point, and ductility of the CCR bitumen are 52.5 dmm, 228 °C, and 85.7 cm, respectively. Figure 1 displays the stiffness modulus of the MA at various temperatures.

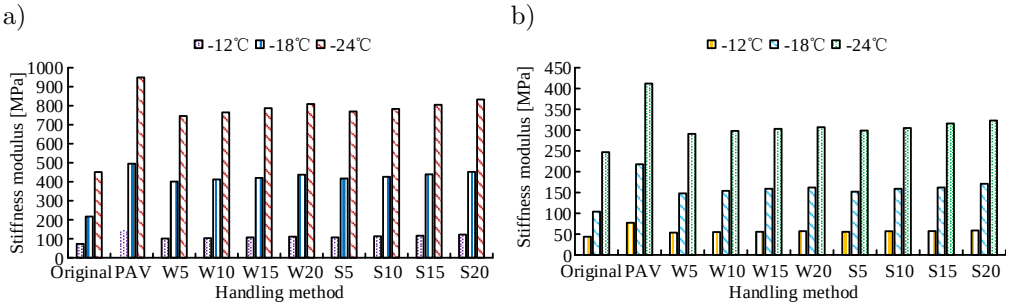

Fig. 1. Stiffness modulus of MA at different temperatures and treatments: a) stiffness modulus of SBS-MA, b) stiffness modulus of CCR-modified asphalt. Note: Wx and Sx represent x FTCs in water and salt solution, respectively.

In Fig. 1a, compared to the virgin SBS bitumen, the stiffness modulus of SBS bitumen after LTA and water/salt FTCs increased significantly and was inversely proportional to the temperature. Among the samples, the PAV-aged SBS bitumen had the largest stiffness modulus, with values of 145 MPa, 495 MPa, and 949 MPa at −12 °C, −18 °C, and −24 °C, respectively. In Fig. 1b, the stiffness modulus of CCR bitumen, after both aging and FTC, increased compared to the original CCR bitumen. Furthermore, as the temperature decreased, the modulus

rose. Among the samples, the PAV-aged CCR bitumen at −24 °C showed the largest stiffness modulus of 412 MPa. Under identical conditions, the stiffness modulus of the CCR bitumen was lower than that of the SBS bitumen. The aforementioned findings suggest that the CCR bitumen has superior LT rheological characteristics compared with the SBS bitumen. Figure 2 depicts the CR of the MA at various temperatures.

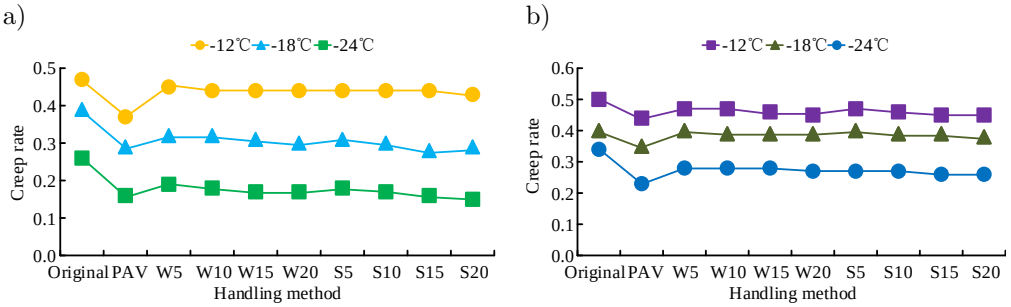

Fig. 2. CR of MA at different temperatures:
a) CR of SBS-MA, b) CR of CCR-MA.

In Fig. 2, the CR of MA, after aging and FTC, decreased compared with the original MA. The most significant reduction in the CR of the aged bitumen was at least 10.9 %. In addition, the CR of the MA decreased as temperature decreased. However, by comparing Fig. 2a and Fig. 2b, it can be observed that the change in the CR of CCR bitumen is relatively small compared to that of SBS bitumen. For example, after the aging treatment, the CR of SBS bitumen and CCR bitumen at −12 °C was 0.37 and 0.44, respectively. These results show that the CCR bitumen has better strain relaxation ability compared with the SBS bitumen. The CR/stiffness modulus ratios of MA at different temperatures are displayed in Table 2.

In Table 2, the CR/stiffness modulus ratios of both SBS bitumen and CCR bitumen decreased significantly after aging and FTC. Taking the PAV-aged bitumen at −12 °C as an example, the CR/stiffness modulus ratios for SBS and CCR bitumen were 257.4 and 571.6, representing reduction of 60.2 % and 49.5 %, respectively. Meanwhile, with the decrease in temperature and the increase in the FTCs, the CR/stiffness modulus ratios of both SBS bitumen and CCR bitumen decreased. In addition, under the same conditions, the CR/stiffness modulus ratio of CCR bitumen was always higher than that of SBS bitumen. For example, at −18 °C, the CR/stiffness modulus ratios of SBS bitumen and CCR bitumen after aging were 58.6 and 160.6, respectively. These results demonstrate that CCR bitumen exhibits excellent LT deformation capability compared with SBS bitumen. Figure 3 displays the infrared spectra of various MA samples before and after aging.

Table 2. CR/stiffness modulus ratio (10^5/MPa) of SBS- and CCR-MAs at different temperatures.

Bitumen type	Processing method	−12 °C	−18 °C	−24 °C
SBS-MA	Original	647.3	179.7	57.6
	PAV	257.4	58.6	16.9
	W5	441.5	79.8	25.5
	W10	429.2	77.7	23.5
	W15	411.4	73.8	21.6
	W20	393.1	68.6	21.0
	S5	414.2	74.3	23.4
	S10	389.6	70.4	21.7
	S15	379.5	63.8	19.9
	S20	355.1	64.2	18.0
CCR-MA	Original	1134.9	384.6	133.6
	PAV	571.6	160.6	55.8
	W5	884.3	270.3	96.2
	W10	849.2	253.2	94.0
	W15	818.5	245.3	92.4
	W20	786.2	240.7	87.9
	S5	846.9	263.2	90.3
	S10	810.4	245.3	88.5
	S15	792.3	240.7	82.3
	S20	761.7	222.2	80.5

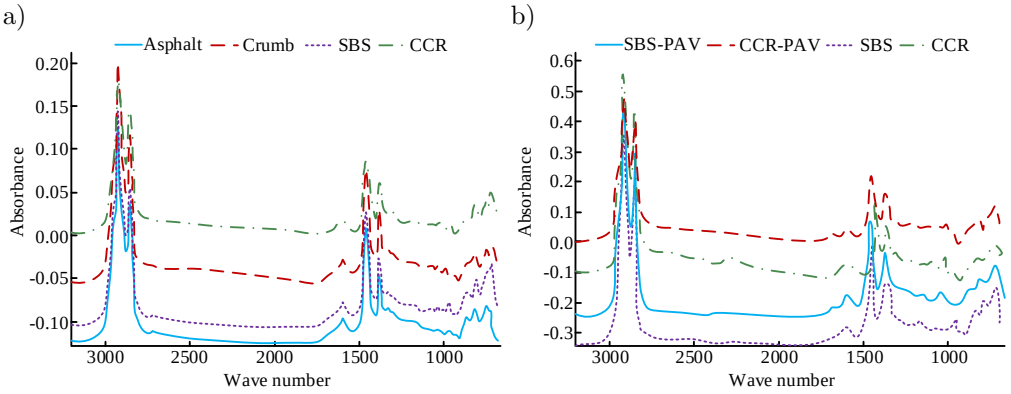

Fig. 3. Infrared spectrum before and after aging of different modified bitumen: a) infrared spectra of asphalt samples, b) infrared spectra of asphalt before and after aging.

In Fig. 3a, the absorption peaks of MaA, crumb rubber MA, SBS bitumen, and CCR bitumen are basically located at the same position, i.e., at wave num-

bers of 2918.2 cm^{-1} and 2849.5 cm^{-1} in the functional group region. All these absorption peaks are generated by the stretching vibration of methylene and its derivatives. Comprehensive analysis suggests that bitumen mainly contains alkanes, cycloalkanes, and aromatic compounds. In Fig. 3b, after aging, the absorbance of both SBS bitumen and CCR bitumen decreased compared with the original samples, with the reduction in the SBS bitumen absorbance being more significant. Among them, the aging SBS bitumen disappeared at a wave number of 966.5, while the aging CCR bitumen's wave peaks did not change significantly. It can be concluded that the polybutadiene and polystyrene of SBS bitumen are decomposed during aging, while there is no significant change in the CCR bitumen. These results indicate that the CCR bitumen has better anti-aging properties than the SBS bitumen. Figure 4 displays the infrared spectra of SBS and CCR bitumen prior to and following FTCs.

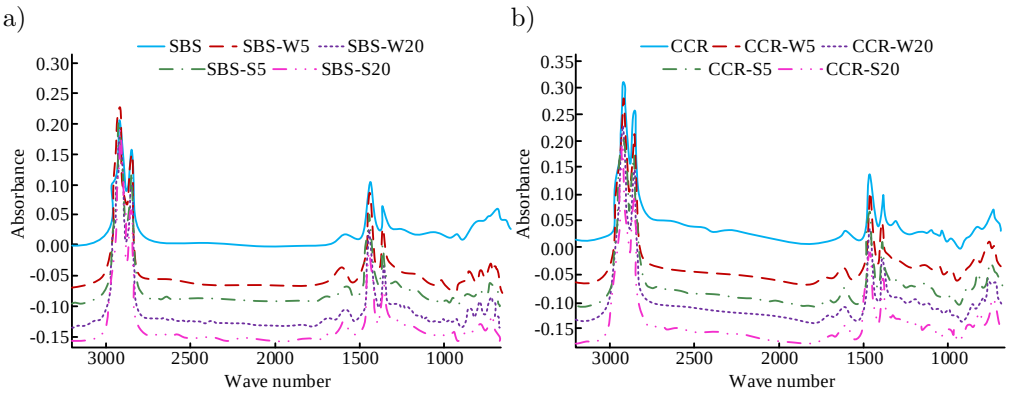

FIG. 4. Infrared spectra of bitumen before and after cyclic FTCs: a) SBS asphalt, b) CCR asphalt.

In Fig. 4a, the absorption peaks of the SBS bitumen at wave numbers of 1599.7 and 1694.6 changed significantly after FTC. This indicates that the aromatic hydrocarbon components of the SBS bitumen changed after FTC. Moreover, both cycloalkanes and unsaturated chains are oxidized, resulting in water-induced aging of the bitumen. In Fig. 4b, the infrared spectral changes of the CCR bitumen after FTC are basically the same as those of SBS bitumen, but the magnitude of change is smaller. This indicates that, compared with the SBS bitumen, the CCR bitumen has better freeze-thaw (FT) resistance. The functional group indices before and after FTC are shown in Fig. 5.

In Fig. 5a, the hydroxyl index of both SBS bitumen and CCR bitumen increased significantly after FTCs. Among them, the hydroxyl index of SBS bitumen is basically above 0.013, while that of CCR bitumen is in the range of 0.010 to 0.012. It can be concluded that the hydroxyl functional group changes

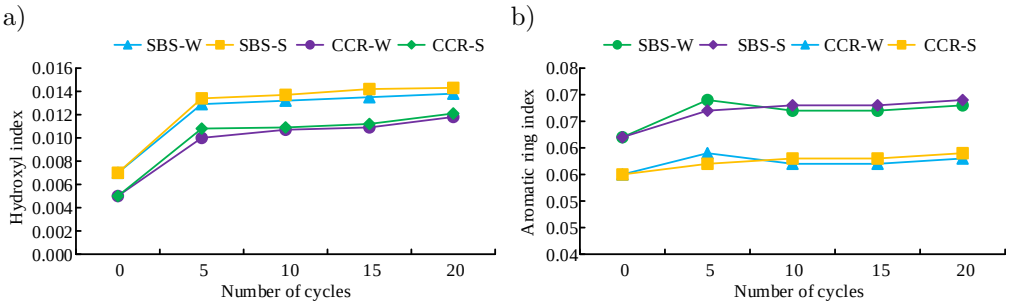

Fig. 5. Functional group indices before and after cyclic FTCs:
a) hydroxyl index, b) aromatic ring index.

of CCR bitumen after FTCs are small. In Fig. 5b, the cycloaromatic index of both SBS bitumen and CCR bitumen also increased significantly after FTCs. Among them, the cycloaromatic indices of two SBS bitumen samples are above 0.065, while those of CCR bitumen are around 0.060. This reveals that FTC have less effect on the cycloaromatic functional groups of the CCR bitumen. In order to investigate the mechanism of changes in the rheological properties of composite-modified bitumen, the microstructure was analyzed using fluorescence microscopy, and the results are shown in Fig. 6.

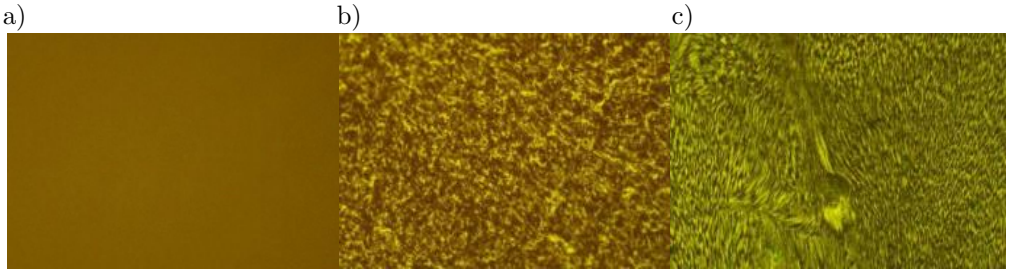

Fig. 6. Fluorescence microscope test results of modified bitumen:
a) matrix asphalt, b) SBS asphalt, c) CCR asphalt.

As shown in Fig. 6, the matrix bitumen appears as a homogeneous phase. SBS has a dense network structure, while SBS particles absorb light oil and expand, rapidly increasing in volume and gradually expanding and splitting, forming a visible network structure that envelops the bitumen in a grid-like structure. However, due to the poor stability of this structure, the modification effect of SBS bitumen is relatively moderate. In the CCR bitumen, rubber powder and SBS are dispersed in the bitumen, and SBS particles serve as anchor points interwoven with the flocculated rubber powder. Together, they form a relatively stable spatial structure, dispersed in the bitumen through coupling, which improves the rheological properties of the bitumen.

3.2. Adhesion characterization of composite MA

To investigate the adhesion properties of MA, the study was conducted to test the contact angle and atomic force to understand the adhesion and the Derjaguin–Muller–Toporov (DMT) modulus of the bitumen. Figure 7 displays the test results of the bitumen contact angle.

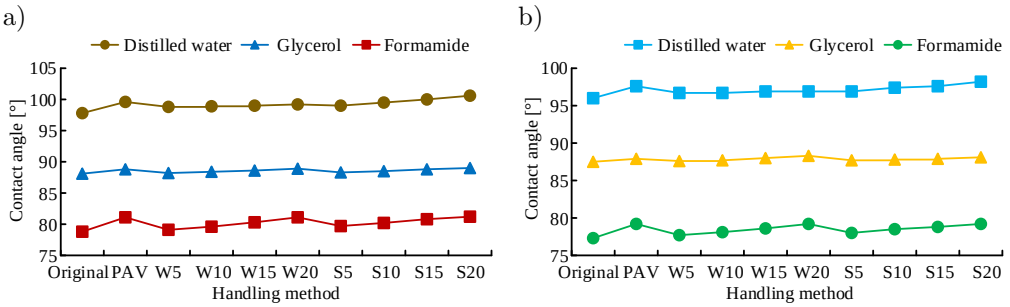

FIG. 7. Test results of the bitumen contact angle:
a) contact angle of SBS asphalt, b) contact angle of CCR asphalt.

In Fig. 7a, the contact angle of SBS bitumen after both aging and FTC is higher than that of the original sample. In the case of distilled water, for example, the contact angles with the original and aged samples are 97.8° and 99.6°, respectively. In Fig. 7b, the contact angles of CCR bitumen are all higher than those of the original samples. Similarly, in the case of distilled water, the contact angles with the original and aged samples are 96.0° and 97.6°, respectively. By comparing SBS-MA and CCR-MA, it is possible to determine that, under identical circumstances, the SBS bitumen has a wider contact angle than the CCR bitumen. With distilled water and ten FTC cycles as an example, the contact angles of SBS and CCR bitumen are 98.9° and 96.7°, respectively. According to the contact angle, the work of adhesion of bitumen can be calculated. Figure 8 presents the findings.

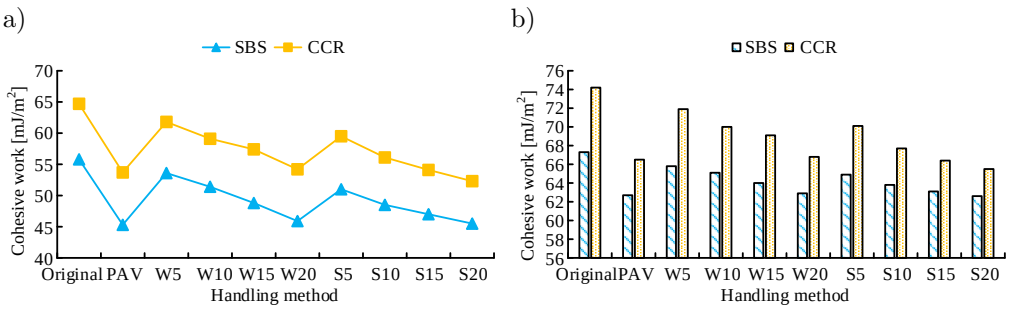

FIG. 8. Cohesion work of bitumen: a) asphalt, b) asphalt and aggregate.

In Fig. 8a, the work of cohesion for the CCR bitumen is higher than that of the SBS bitumen under the same conditions. For example, the cohesive polymerization function of SBS bitumen and CCR bitumen after five FTCs is 53.6 mJ/m^2 and 61.8 mJ/m^2, respectively. In Fig. 8b, the cohesive polymerization function between CCR bitumen and aggregate is higher than that of SBS bitumen under the same conditions. Taking the aged bitumen as an example, the work of adhesion between SBS bitumen and aggregate and between CCR bitumen and aggregate is 62.7 mJ/m^2 and 66.5 mJ/m^2, respectively. The microscopic adhesion and the DMT modulus of the bitumen are shown in Fig. 9.

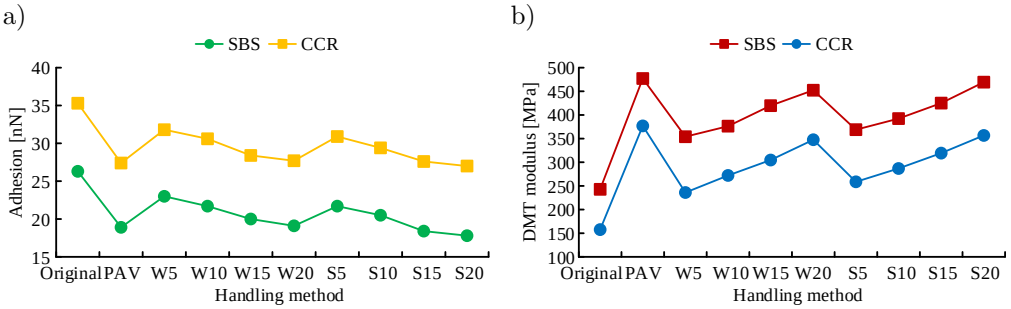

Fig. 9. Microscopic adhesion force (a) and DMT modulus (b) of bitumen.

In Fig. 9a, the adhesion force of bitumen is significantly reduced after treatment by either aging or FTC. In addition, the adhesion force of the CCR bitumen is greater under the same conditions. For example, the adhesion forces of SBS bitumen and CCR bitumen after aging are 18.9 nN and 27.4 nN, respectively. In Fig. 9b, the DMT modulus of the bitumen is significantly reduced after treatment by aging or FTC. Moreover, the DMT modulus of the CCR bitumen is smaller under the same conditions. For example, after five FTCs, the DMT moduli of SBS bitumen and CCR bitumen are 354.0 MPa and 236.0 MPa, respectively. These results indicate that the CCR bitumen has better cracking, aging and FT resistance. In order to investigate the mechanism of changes in CCR bitumen performance, the phase structure of the modified bitumen was analyzed using scanning electron microscopy, and the results are shown in Fig. 10.

As shown in Fig. 10, the surface of the matrix bitumen is smooth and free of impurities, with a linear morphology that is close to a homogeneous structure. In the SBS-modified bitumen, the SBS modifier is in a dispersed phase; however, due to the difficulty of forming a stable structural system between the SBS particles and the bitumen, the modification effect is relatively average. In the CCR-modified bitumen, the particle distribution of the modifier is denser, and a thicker gel-like substance is formed at the interface, which indicates that the rubber powder and SBS undergo sufficient vulcanization and swelling reactions

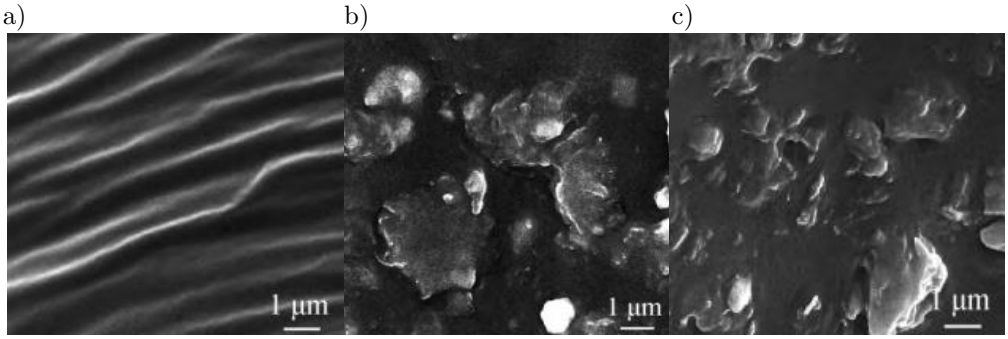

FIG. 10. Scanning electron microscope images:
a) matrix asphalt, b) SBS-MA, c) CCR-MA.

in the bitumen. This enhances the tensile deformation resistance and elastic recovery ability of the bitumen under external force.

3.3. LT cracking characterization of composite MA *mixes*

The study used both TPBTs and CSTS tests to evaluate the LT cracking properties of MA mixes. The results of the restrained specimen temperature stress test are shown in Fig. 11.

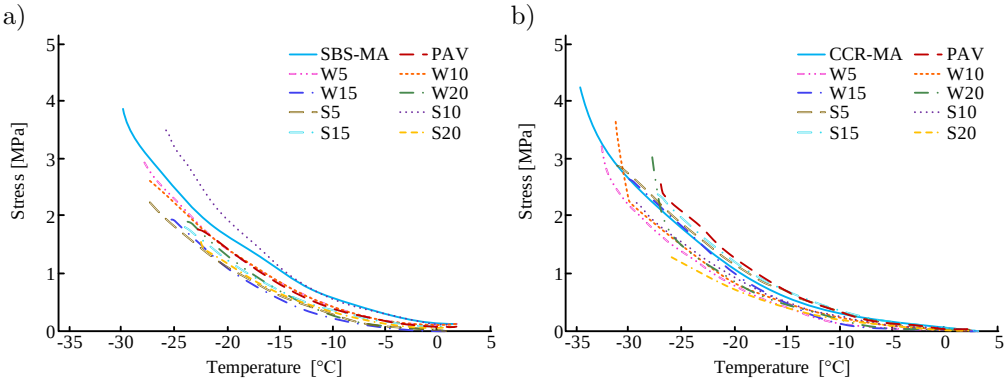

FIG. 11. Results of the temperature stress test on restrained specimens for:
a) SBS-MA, b) CCR-MA.

In Fig. 11a, the freeze-off temperatures of AMs after aging and FTC are significantly higher compared with those of the original SBS-AMs. The FT temperatures of SBS-MA mixture (SBS-MA), SBS-MA-PAV, and SBS-MA-W5 are −30 °C, −22.5 °C, and −27.7 °C, respectively. In Fig. 11b, the freeze-off temperatures of CCR-AMs are also significantly increased after aging and FTC. The FT temperatures of CCR-MA mixture (CCR-MA), CCR-MA-PAV and CCR-MA-W5 are −34.3 °C, −27.1 °C, and −32.5 °C, respectively, which are lower than

those of SBS-AMs. The aforementioned findings suggest that the CCR bitumen better resists LT cracking. Figure 12 displays the TPBT results of the beams.

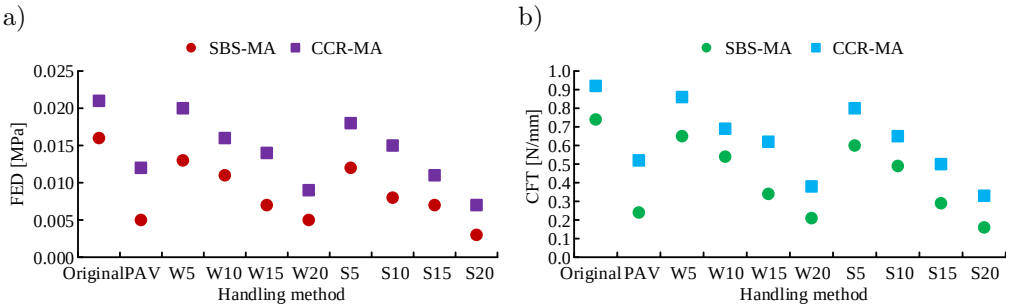

Fig. 12. TPBT results of small beams: a) FED, b) critical fracture toughness (CFT).

In Fig. 12a, the FEDs of AMs are significantly reduced after both aging and FTC. However, the FED of CCR-AMs is higher than that of SBS-AMs. For example, the FEDs of SBS-MA-PAV and CCR-PAV are 0.005 MPa and 0.012 MPa, respectively. In Fig. 12b, the CFT of AMs is significantly reduced after both aging and FTC. However, the CFT of CCR-AMs is higher under the same conditions. For example, the CFTs of SBS-MA-PAV and CCR-PAV are 0.24 N/mm and 0.52 N/mm, respectively. These results indicate that CCR bitumen has better toughness and cracking resistance. The study statistically analyzes the FED and CFT in order to understand the sensitivity of these parameters to each of the influencing factors. The sensitivities of the influencing factors are shown in Table 3.

Table 3. Sensitivity of influencing factors.

Influence factor	Index	Coefficient of variation [%]
Preburning	Fracture energy density	0.42
	Critical fracture toughness	0.39
FTC	Fracture energy density	0.37
	Critical fracture toughness	0.36
FT type	Fracture energy density	0.09
	Critical fracture toughness	0.07
Types of bitumen	Fracture energy density	0.27
	Critical fracture toughness	0.22

In Table 3, both FED and CFT are most sensitive to aging, with coefficients of variation (COVs) of 0.42 and 0.39, respectively. The next most sensitive factor is the number of FT cycles, with COVs of 0.37 and 0.36, respectively. In addition,

both FED and CFT are least sensitive to FT type, with COVs of 0.09 and 0.07, respectively. The results of the rutting test are shown in Fig. 13.

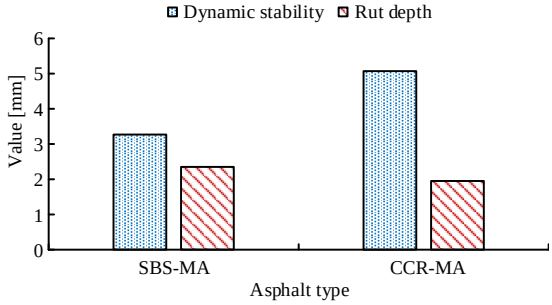

FIG. 13. Track test results.

As shown in Fig. 13, compared to SBS-MA, CCR-MA has greater dynamic stability and smaller rut depth. The dynamic stability of SBS-MA and CCR-MA is 3.27 times/mm and 5.07 times/mm, respectively, and the rut depths are 2.35 mm and 1.94 mm, respectively. These results indicate that the rubber-powder composite SBS can effectively improve the deformation resistance of bitumen materials. In terms of economic benefits, although SBS-modified bitumen has good road performance, its high cost limits its large-scale application. CCR composite-modified bitumen can reduce the amount of SBS modifier while maintaining bitumen performance by adding rubber powder, thus lowering production costs.

4. Discussion

A composite MA-CCR bitumen based on crumb rubber and an SBS modifier was created, and its rheological characteristics and LT cracking capabilities were examined in order to extend the life of AP and lower the likelihood of its cracking under LT conditions. The experimental results indicated that both SBS bitumen and CCR bitumen exhibited a significant increase in the stiffness modulus after aging and FTC. Furthermore, as the temperature dropped, the stiffness modulus rose. However, compared to SBS bitumen, the stiffness modulus of CCR bitumen under the same conditions was smaller.

Taking the aged bitumen as an example, the stiffness modulus of SBS bitumen and CCR bitumen at −24 °C was 949 MPa and 412 MPa, respectively. Furthermore, the change in the CR of CCR bitumen was negligible in comparison to that of SBS bitumen. Using aged bitumen as an example, the CR values at −12 °C were 0.37 and 0.44 for SBS and CCR bitumen, respectively. This suggests that the CCR bitumen has a higher capability for strain relaxation compared to the SBS bitumen.

Compared to the MA based on nano ZnO and SBS proposed by Li *et al.* [15], the MA with CCR exhibited better FTC resistance and creep performance. Specifically, the creep performance of the MA based on nano ZnO and SBS was improved by about 5 % compared to that of the SBS MA, whereas the creep performance of CCR-MA improved by about 19 % compared with the SBS bitumen. This improvement was due to the mixing and solubilization between the SBS modifier, crumb rubber modifier, and bitumen, which resulted in a physical cross-linking structure [16, 17].

An investigation of the infrared spectra of various bitumen was carried out in order to better understand the mechanism underlying the changes in MA properties. The outcomes indicated that SBS bitumen and CCR bitumen mainly contained alkanes, cycloalkanes and aromatic compounds. After aging, the absorbance of both SBS bitumen and CCR bitumen decreased compared with the original samples, with the decrease in SBS bitumen absorbance being more pronounced. Specifically, the wave peak of aged SBS bitumen disappeared at a wave number of 966.5, while the wave peak of aged CCR bitumen did not change significantly. It can be concluded that the polybutadiene and polystyrene in aged SBS bitumen were decomposed. This led to an increase in the content of hydroxyl, aromatic ring, and sulfinyl groups, which weakened its LT performance, while there was no significant change in CCR bitumen. After FTC, the aromatic hydrocarbon fractions of both SBS and CCR bitumen changed. Moreover, both the cycloalkanes and unsaturated chains were oxidized, which caused water aging of the bitumen; the degree of water aging of CCR bitumen was smaller [18].

In addition, fluorescence microscopy results showed that, compared to the SBS-modified bitumen, in the CCR-modified bitumen, SBS particles serve as anchor points interwoven with flocculated rubber powder, and the two form a relatively stable spatial structure dispersed in bitumen through coupling, thereby improving the rheological properties of the bitumen. At the same time, scanning electron microscopy revealed that in the CCR-modified bitumen, the particle distribution of modifier was denser, and a thicker gel-like material was formed at the interface. This indicates that the rubber powder and SBS undergo sufficient vulcanization and swelling reactions in bitumen, enhancing the tensile deformation resistance and elastic recovery ability of the bitumen under external forces.

To investigate the adhesion properties of the MA and the LT characteristics of its mixtures, the study conducted contact angle and atomic force tests, as well as CSTS tests and TPBTs. The findings showed that the cohesion function of the MA was reduced after both aging and FTC; however, under the same conditions, the cohesion function of CCR bitumen was higher than that of SSB bitumen. For example, the cohesive polymerization function of SSB bitumen and CCR bitumen after five water FTCs was 53.6 $\mathrm{mJ/m^2}$ and 61.8 $\mathrm{mJ/m^2}$, respectively.

Meanwhile, the DMT modulus of bitumen was significantly reduced after aging or FTC treatment. Moreover, the DMT modulus of CCR bitumen was smaller under the same conditions. Taking five water FTCs as an example, the DMT modulus of SBS bitumen and CCR bitumen was 354.0 MPa and 236.0 MPa, respectively. This is because aging and FTC would convert viscous components of bitumen into elastic components, leading to reduction of its deformation ability. SBS and crumb rubber in CCR bitumen reduce the effects of temperature, water, salts, and other factors on the viscous component, so the CCR bitumen exhibits better deformation capacity [19, 20].

Through comparison with Yang *et al.* [21], it can be observed that after FTC, there was a noticeable increase in surface cracking in bitumen cold-recycled mixtures, along with an increase in the width and number of main cracks. In addition, this observation is supported by the progressive decrease in the fatigue life (number of cycles) at the full-field maximum horizontal strain and the notable increase in the average volume of air voids and intermediate voids. Similarly, the results of Wang *et al.* [22] also demonstrated that after FTC, the mechanical properties of AMs were greatly reduced and key particles in the AM structure were significantly displaced.

The FED and CFT of the AMs decreased significantly after aging and FTC, while the freeze-fracture temperature increased significantly. This was due to the fact that aging increased the polar components in the bitumen, making it more prone to fracture. Meanwhile, freezing pressure generated by freezing and thawing increased the porosity of AMs, allowing liquids to enter the pore interior. Additionally, upon thawing, positive pressure occurred, which consequently caused the AM's strength to decrease. In terms of LT cracking, CCR-AMs outperformed SBS-AMs. This is attributed to CCR-AMs' superior ability to release stress in the form of deformation, and the higher energy required for crack propagation.

5. Conclusion

This study proposed a composite MA based on SBS and crumb rubber to improve the frost resistance of APs, and evaluated the MA's performance. The results showed that after LTA and water/salt FTCs, the CR of the MA decreased. Among these, the CR of aged bitumen was reduced most significantly, by at least 10.9 %. In addition, the CR of the MA decreased with decreasing temperature. However, compared with the SBS bitumen, the change in the CR of the CCR bitumen was relatively small. Taking the bitumen after the aging treatment as an example, the CR of SBS bitumen and CCR bitumen at −12 °C was 0.37 and 0.44, respectively.

In addition, the freeze-off temperatures of AMs after aging and FTC increased significantly, but the freeze-off temperature of CCR-AMs was always higher than that of SBS-AMs. For example, the freeze-off temperatures of SBS-MA-W5 and CCR-MA-W5 were $-27.7\,^{\circ}\mathrm{C}$ and $-32.5\,^{\circ}\mathrm{C}$, respectively. These results indicate that CCR bitumen has good rheological properties and excellent LT cracking resistance.

CCR composite-modified bitumen can be applied in highway pavement construction to improve road durability and service life due to its excellent HT stability and LT crack resistance. At the same time, the composite-modified bitumen can also be used for waterproof and anti-corrosion coatings on breakwaters and piers to resist seawater erosion.

The current study only analyzed the performance of CCR bitumen with a single SBS and rubber powder content, which limits the comprehensiveness of the research results. Future research will expand to CCR bitumen with different doping levels, systematically analyzing the effects of different proportions of rubber powder and SBS on bitumen performance to determine the optimal mixing ratio. This will help optimize the mechanical properties and durability of bitumen while reducing costs and providing a scientific basis for the widespread application of bitumen pavements.

Fundings

The research was supported by National Natural Science Foundation of China, 'Decaying prediction of aging performance of hot recycled asphalt and mixture under exposure situation in Northwest, China' (no. 52268070), and Research project of Gansu Provincial Department of Transportation, 'Evaluation and application of aging resistance of thermal reclaimed bitumen pavement in Gansu Province' (no. 2023-02).

Conflicting interest

The authors declare that they have no known competing financial interests or personal relationships that could have appeared to influence the work reported in this paper.

Authors' contributions

All authors contributed equally to this work, reviewed, and approved the final manuscript.

References

1. Kumar Y., Kumar P., Ravindranath S.S., Evaluating the intermediate temperature properties of SB modified asphalt binders: Influence of SB copolymer structure,

International Journal of Pavement Research and Technology, **17**(4): 1014–1031, 2024, https://doi.org/10.1007/s42947-023-00283-1.

2. Wei Z., Zhao Z., Hui C., Junjie X., Huaxin X., Dongyu N., High temperature rheological properties of surface pretreated PVA fiber modified asphalt [in Chinese], *Journal of Shenzhen University Science and Engineering*, **39**(4): 409–416, 2022, https://doi.org/10.3724/sp.j.1249.2022.04409.

3. Rahman M.N., Sarkar M.T.A., Elseifi M.A., Mayeux C., Cooper S.B., Free K., Short-term field performance and cost-effectiveness of crumb-rubber modified asphalt emulsion in chip seal applications, *Transportation Research Record*, **2675**(9): 1049–1062, 2021, https://doi.org/10.1177/03611981211005469.

4. Elmoghazy Y., Abuelgasim E.M.O., Osman S.A., Afaneh Y.R.H., Eissa O.M.A., Safaei B., Effective mechanical properties evaluation of unidirectional and bidirectional composites using virtual domain approach at microscale, *Archives of Advanced Engineering Science*, **1**(1): 27–37, 2023, https://doi.org/10.47852/bonviewAAES32021723.

5. Liu B., Li X., Li S., Pavement performance analysis of carbon nanotube/SBS composite modified asphalt, *Carbon Letters*, **34**(1): 343–350, 2024, https://doi.org/10.1007/s42823-023-00605-0.

6. Ting J.H., Khare E., DeBellis A., Orr B., Jourdan J.S., Martín-Martínez F.J., Jin K., Malonson B.L., Buehler M.J., Role of methylene diphenyl diisocyanate (MDI) additives on SBS-modified asphalt with improved thermal stability and mechanical performance, *Energy & Fuels*, **35**(21): 17629–17641, 2021, https://doi.org/10.1021/acs.energyfuels.1c02794.

7. Duarte Mendonça A.M.G., Melo Neto O. de M., Rodrigues J.K.G., Batista de Lima R.K., Silva I.M., Marques A.T., Characterisation of modified asphalt mixtures with lignin of *pinus* and *eucalyptus* woods, *Australian Journal of Civil Engineering*, **21**(2): 253–264, 2023, https://doi.org/10.1080/14488353.2022.2089376.

8. Li H., Sun J., Wang S., Zhang M., Hu Y., Sheng Y., Bamboo fiber modified asphalt mixture proportion design and road performances based on response surface method, *Journal of Wuhan University of Technology-Materials Science Edition*, **38**(1): 156–170, 2023, https://doi.org/10.1007/s11595-023-2678-8.

9. Amini N., Hayati P., Latifi H., Evaluation of rutting and fatigue behavior of modified asphalt binders with nanocomposite phase change materials, *International Journal of Pavement Research and Technology*, **16**(3): 678–692, 2023, https://doi.org/10.1007/s42947-022-00156-z.

10. Chen S., Wang Y., He X., Su Y., Pan Y., Cao Y., Wang W., Yang C., Jiang B., Zhang S., Viscous flow activation energy and short-term aging resistance of SBS-modified asphalt enhanced by PPA oil-grinding activated MoS_2, *Fluid Dynamics and Materials Processing*, **21**(2): 387–404, 2025, https://doi.org/10.32604/fdmp.2024.055697.

11. Li C., Ma F., Fu Z., Dai J., Wen Y., Wang Y., Rheological behavior of polyphosphoric acid-vulcanized liquid rubber compound modified asphalt binder, *Iranian Journal of Science and Technology, Transactions of Civil Engineering*, **46**(5): 3931–3945, 2022, https://doi.org/10.1007/s40996-022-00831-y.

12. Song W., Study on the high and low temperature performance of nano alumina modified asphalt mixture, *International Journal of Microstructure and Materials Properties*, **16**(4): 229–238, 2022, https://doi.org/10.1504/IJMMP.2023.128421.

13. Enieb M., Cengizhan A., Karahancer S., Eltwati A., Evaluation of physical-rheological properties of nano titanium dioxide modified asphalt binder and rutting resistance of modified mixture, *International Journal of Pavement Research and Technology*, **16**(2): 285–303, 2022, https://doi.org/10.1007/s42947-021-00131-0.

14. Habbouche J., Piratheepan M., Hajj E.Y., Bista S., Sebaaly P.E., Full-scale pavement testing of a high polymer-modified asphalt concrete mixture, *Journal of Testing and Evaluation*, **50**(2): 865–888, 2022, https://doi.org/10.1520/JTE20210283.

15. Li X., Shen J., Dai Z., Ling T., Li X., Comprehensive performances of hybrid-modified asphalt mixtures with nano-ZnO and styrene-butadiene-styrene (SBS) modifiers, *The Baltic Journal of Road and Bridge Engineering*, **17**(3): 170–186, 2022, https://doi.org/10.7250/bjrbe.2022-17.574.

16. Hao H., Chen Z., Cong P., Han Z., Rheological, chemical and short-term aging properties of waste polyurethane particles modified asphalt binder with or without SBS, *Construction and Building Materials*, **357**: 129363, 2022, https://doi.org/10.1016/j.conbuildmat.2022.129363.

17. Zeng J., Zhao J., Mechanism and performance investigation of SBS/sulfur composite modified asphalt, *Petroleum Chemistry*, **62**(7): 732–739, 2022, https://doi.org/10.1134/S0965544122050140.

18. Otto C.G., Awarri A.W., Comparative cost-effectiveness of modified asphalt concrete submerged in moisture as related to fatigue performance, *IOSR Journal of Mechanical and Civil Engineering*, **18**(2): 49–54, 2021.

19. Tiza M., Duweni C., Mogbo O., Terlumun S., Asawa J., Characterization of reclaimed asphalt pavement and optimization in polymer modified asphalt blends: A review, *Civil Engineering Beyond Limits*, **2**(2): 27–34, 2021, https://doi.org/10.36937/cebel.2021.002.004.

20. Cong P., Guo X., Mei L., Zhang Y., Influences of aging on the properties of SBS-modified asphalt binder with anti-aging agents, *Iranian Journal of Science and Technology, Transactions of Civil Engineering*, **46**(2): 1571–1588, 2021, https://doi.org/10.1007/s40996-021-00650-7.

21. Yang Y., Yue L., Yang Y., Chen Y.Y., Multi-scale decay mechanism of emulsified asphalt cold recycled mixture under freeze-thaw, *The Baltic Journal of Road and Bridge Engineering*, **18**(3): 50–69, 2023, https://doi.org/10.7250/bjrbe.2023-18.608.

22. Wang N., Zhang H., Xiong H., Microstructure and mechanical behavior of asphalt mixture based on freeze-thaw cycle, *Multidiscipline Modeling in Materials and Structures*, **17**(4): 760–774, 2021, https://doi.org/10.1108/MMMS-10-2020-0262.

Received April 27, 2025; revised July 7, 2025; accepted July 11, 2025; available online December 18, 2025; version of record March 17, 2026; published issue March 30, 2026.